Molecular Architecture with 2,2′-Bipyrazine and Metal Ions: Infinite Loop and Molecular Square

Ralf-Dieter Schnebeck,[a] Eva Freisinger,[a] and Bernhard Lippert*[a]

Dedicated to Professor Heinrich Vahrenkamp on the occasion of his 60th birthday

Keywords: N ligands / Palladium / Platinum / Silver / Molecular architecture / Structure elucidation

The potential of $[L_2Pd(2,2'\text{-bpz-}N^1,N^{1'})]^{2+}$ [L_2 = en (**1**), L = H_2O (**4a**), 2,2′-bpz = 2,2′-bipyrazine] for use as an angular element in the generation of self-organized systems of variable molecular architecture has been studied. Ag^+ forms an infinite loop **3** with **1**, in which the metal ions function as cross-linking agents between the organic entities 2,2′-bpz. Complex **4a**, on the other hand, self-assembles as a bis(μ-OH) dinuclear species **4b**, and in the presence of 4,4′-bipyridine (4,4′-bpy) as a molecular square **6** with the heteroaromatic 4,4′-bpy ligands representing the cross-linking entities.

Introduction

The generation of regularly shaped molecules ("molecular architecture") from organic ligands and metal entities is an area of great current interest.[1] Our own activities in this field have centered on combinations of linear (*trans*-a_2Pt^{II} with a = NH_3 or CH_3NH_2; Hg^{2+}) or *cis*-square planar (*cis*-a_2Pt^{II}, $enPt^{II}$, $enPd^{II}$) metal fragments and nucleobases or other heterocyclic ligands.[2] Among others, we have been able to isolate and characterize molecular rectangles,[3] hexagons,[4] open boxes,[4,5] triangles,[6] and barrels.[7] The use of 2,2′-bipyrazine (2,2′-bpz) proved to be particularly fortunate since it provided a large number of different metal-binding patterns due to the availability of four ring N donor atoms and its structural flexibility about the central C2−C2′ bond (Scheme 1).

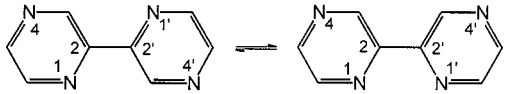

Scheme 1

Interestingly, $enPd^{II}$ forms a mononuclear chelate with 2,2′-bpz, $[enPd(2,2'\text{-bpz-}N^1,N^{1'})]^{2+}$ (**1**),[6a] whereas under comparable conditions $enPt^{II}$ forms a cyclic trinuclear structure, $[\{enPt(2,2'\text{-bpz-}N^4,N^{4'})\}_3]^{6+}$,[7] which is to be considered the kinetic product of this reaction. It can be converted into the analogous chelate with *N*(1),*N*(1′)− metal binding on prolonged heating.[7] The triangle can exist as different conformers, depending on the mutual orientation of the two pyrazine moieties of the 2,2′-bpz ligand.[7] Both the mononuclear Pd complex[6] and the Pt triangle[6a,7] can be applied as building blocks for larger aggregates by combining them with suitable metal fragments. For example, three $[enPd(2,2'\text{-bpz-}N^1,N^{1'})]^{2+}$ cations and three *trans*-$(NH_3)_2Pt^{II}$ units form a flat triangle **2** with Pd^{II} at the corners and Pt^{II} in the middle of the sides of the triangle,[6c] whereas combination of the Pt triangle $[\{enPt(2,2'\text{-bpz-}N^4,N^{4'})\}_3]^{6+}$ with three $enPd^{II}$ yields a hexanuclear molecular vase[6b] or with three Ag^+, a container compound.[7] Anion inclusion is a general phenomenon of all these compounds.

In continuation of this work we report herein the product obtained by cocrystallizing **1** with $AgClO_4$, as well as our efforts to prepare *cis*-$[(H_2O)_2M(2,2'\text{-bpz-}N^1,N^{1'})]^{2+}$ (M = Pd^{II}, Pt^{II}) instead of coordinatively saturated $[enPd(bpz\text{-}N^1,N^{1'})]^{2+}$ species and to probe their use as building blocks for regularly shaped macrocyclic compounds.

Results and Discussion

Infinite Loop Structure

As mentioned in the introduction, $[enPd(2,2'\text{-bpz-}N^1,N^{1'})]^{2+}$ (**1**) forms a triangle **2** with *trans*-$[(NH_3)_2Pt(H_2O)_2]^{2+}$, with the bpz ligands essentially coplanar with the six metal ions (Scheme 2).[6c] Although **2** forms an arrangement in the solid state that gives rise to a channel with a string of ClO_4^- anions in its center, the presence of the NH_3 ligands at Pt^{II} and their orientation essentially perpendicular to the plane of the triangle precludes any direct stacking of the cations. Rather, counter anions and water molecules are assisting formation of the channel. An obvious idea was to apply linearly coordinated metal ions such as Ag^+ instead of *trans*-$(NH_3)_2Pt^{II}$ in order to achieve neat stacking of the 2,2′-bpz entities. At the same time the use of Ag^+ instead of Pt^{2+} would somewhat reduce the high positive charge of the hexanuclear cation. However, the experiment carried out with $AgClO_4$ did not yield the anticipated closed triangular structure and neither did it generate a helical nor a polymeric open zigzag chain. Rather, as revealed by X-ray crystallography, an infinite loop is formed.

Figure 1 provides different views of the polymeric structure of $\{[enPd(2,2'\text{-bpz})Ag](ClO_4)_3\}_\infty$ (**3**). Selected bond

[a] Fachbereich Chemie, Universität Dortmund,
44221 Dortmund, Germany
Fax: (internat.) + 49-(0)231/755-3797

  1434−1948/00/0606−1193 $ 17.50+.50/0

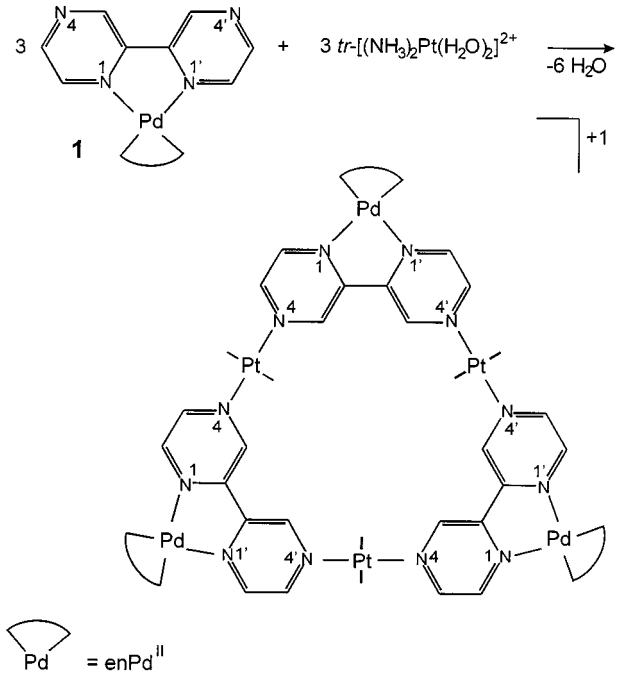

Scheme 2

lengths and angles of **3** are listed in Table 1. The geometry of the enPd(2,2′-bpz) moiety is normal.[6a] Ag(1) cross-links two [enPd(2,2′-bpz-N^1,$N^{1'}$)]$^{2+}$ fragments via two N(4) positions in a linear fashion, whereas there is a 160.4(3)° angle about Ag(2). It appears 1that deviation from linearity about the second silver ion is caused by the asymmetry of weak Ag(2)···$OClO_3^-$ interactions (Figure 2). The two enPd(2,2′-bpz) units bound to Ag(1) are coplanar, but those bound to Ag(2) form a dihedral angle of 30.5(2)°. As a consequence, Pd−Pd distances across Ag(1) are longer [13.930(2) Å] than those across Ag(2) [13.542(3) Å], and likewise distances between the Ag centers differ [Ag(1)···Ag(1′), 6.780(2) Å; Ag(2)···Ag(2′), 13.559(3) Å]. As evident from Figure 1, the respective metal cations are arranged in a collinear fashion along the *x* axis.

Table 1. Selected bond lengths [Å] and angles [°] of **3**

Pd(1)−N(1)	2.020(5)	N(1)−Pd(1)−N(12)	177.3(2)
Pd(1)−N(12)	2.025(5)	N(1)−Pd(1)−N(11)	98.2(2)
Pd(1)−N(11)	2.027(5)	N(12)−Pd(1)−N(11)	82.7(2)
Pd(1)−N(1′)	2.035(4)	N(1)−Pd(1)−N(1′)	80.3(2)
Ag(1)−N(4)	2.202(5)	N(12)−Pd(1)−N(1′)	98.8(2)
Ag(2)−N(4′)	2.200(4)	N(11)−Pd(1)−N(1′)	178.4(2)
		N(4)[a]−Ag(1)−N(4)	180
		N(4′)[b]−Ag(2)−N(4′)	160.4(3)

Symmetry operation: [a] $-x+1, -y, -z$. − [b] $-x+1, y, -z-1/2$.

Triangle vs. Alternatives

Reaction of **1** with Ag^+ can, in principle, lead to a triangle, an infinite helix, an infinite zigzag chain, or an infinite loop (Scheme 3). Formation of monomeric species with PdAg or $PdAg_2$ stoichiometry is not considered here. With $AgClO_4$ the loop structure is exclusively formed. Inspection of the solid state structure reveals why **3**, unlike the structurally related Pd_3Pt_3 compound **2**, does not from a triangle. At the same time it provides clues regarding the re-

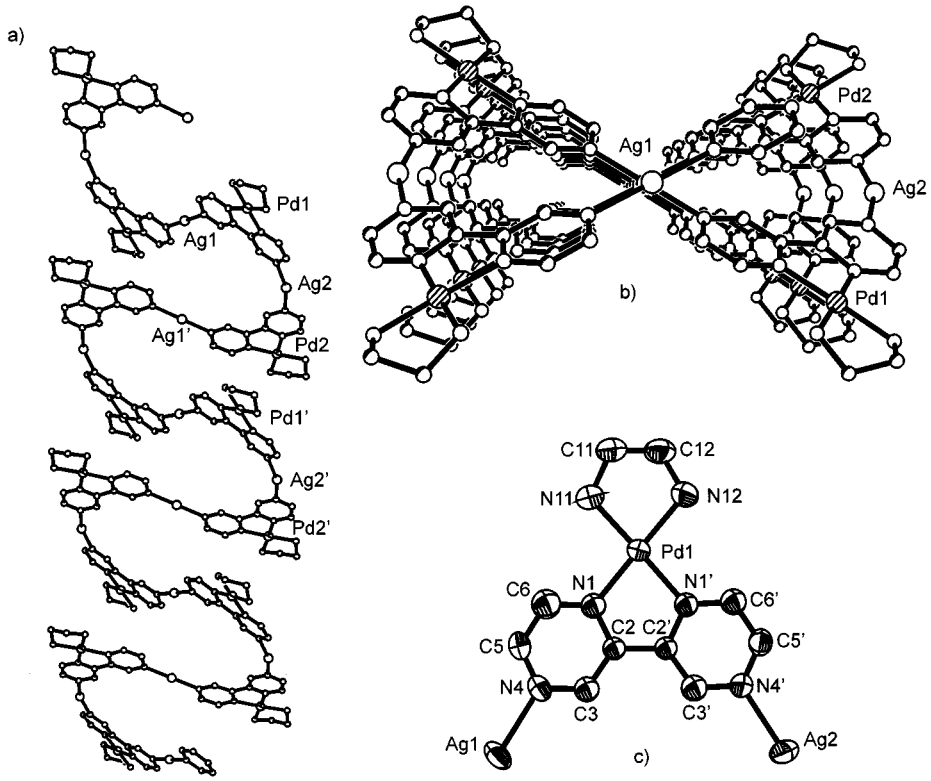

Figure 1. Side view (a), view along the *x* axis (b), and view of a section of [enPd(2,2′-bpz)Ag](ClO$_4$)$_3$ (**3**) (c); central Ag(1) ions are 6.780(2) Å apart, outer Ag(2) as well as Pd(1) ions are 13.559(3) Å apart, which correspond to the length of the crystallographic *c* axis

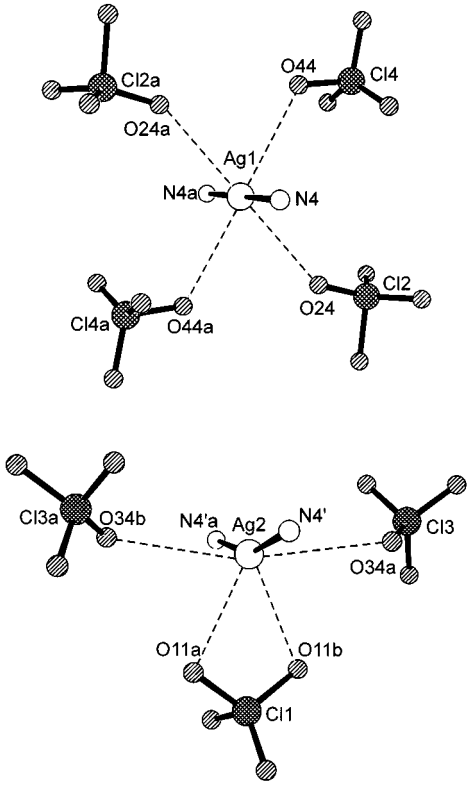

Figure 2. Different environments of Ag(1) and Ag(2) ions; Ag···O contacts are as follows: Ag(1)···O(44), 2.770(7) Å; Ag(2)···O(34a), 2.96(2) Å; Ag(2)···O(11a), 2.71(2) Å; Ag(1)···O(24), 2.71(2) Å

quirements for formation of all four feasible arrangements. There are two geometrical features that prevent closure of a Pd_3Ag_3 combination to form a triangle: First, the loss of coplanarity of the enPd(2,2′-bpz) entities cross-linked by Ag(2). Second, the *head-tail* orientation of the two enPd(2,2′-bpz) entities cross-linked by Ag(1). For formation of a closed triangle, mutual *head-head* orientation of all three enPd(2,2′-bpz) units is absolutely essential. It appears that the loss of collinearity about Ag(2) is of less importance, even though it might facilitate the propeller twist, hence loss of coplanarity of the two bpz ligands bound to Ag(2). The two geometrical parameters mentioned above therefore determine which of the three possible alternatives to the triangle is formed (Table 2).

Table 2. Relationship between possible structures derived from [enPd(2,2′-bpz- N^1,$N^{1'}$)]$^{2+}$ and linear metal entities from geometrical parameters

Structure	Angles [°] between three adjacent bpz ligands	Mutual orientation of adjacent bpz ligands
Triangle	ca. 0	all *head-head*
1D helix	at least 1 angle ≠ 0	all *head-head*
Loop	at least 1 angle ≠ 0	1 *head-tail*
Zigzag chain	0 or ≠ 0	all *head-tail*

We suspect that in addition to concentration effects, which should favor formation of a triangle in more dilute solution and of polymeric structures in concentrated solution, the role of the anions may be crucial in determining the solid-state structure. Although we have varied the Ag salts ($AgNO_3$, $AgPF_6$), we were unable to obtain crystals of sufficient quality for X-ray analysis with NO_3^- and PF_6^- anions. According to ^{1}H-NMR spectroscopy, **3** is labile in aqueous solution and dissociates into **1**, Ag^+, and ClO_4^-. Crystallization thus necessarily occurs from a concentrated solution, thereby favoring a polymeric structure. We note that polymeric helical structures are quite common in systems comprised of heterocyclic N-donor ligands, Ag^+ ions and poorly coordinating anions.[8] There is also an interesting parallel in the literature between our previously described Pd_3Pt_3 triangle[6c] and the polymeric PdAg structure of **3**: Kim et al.[9] have described a molecular triangle comprised of $enPt^{II}$ corners and sides that consist of pseudorotaxanes [cucurbituril entity treaded by the bifunctional

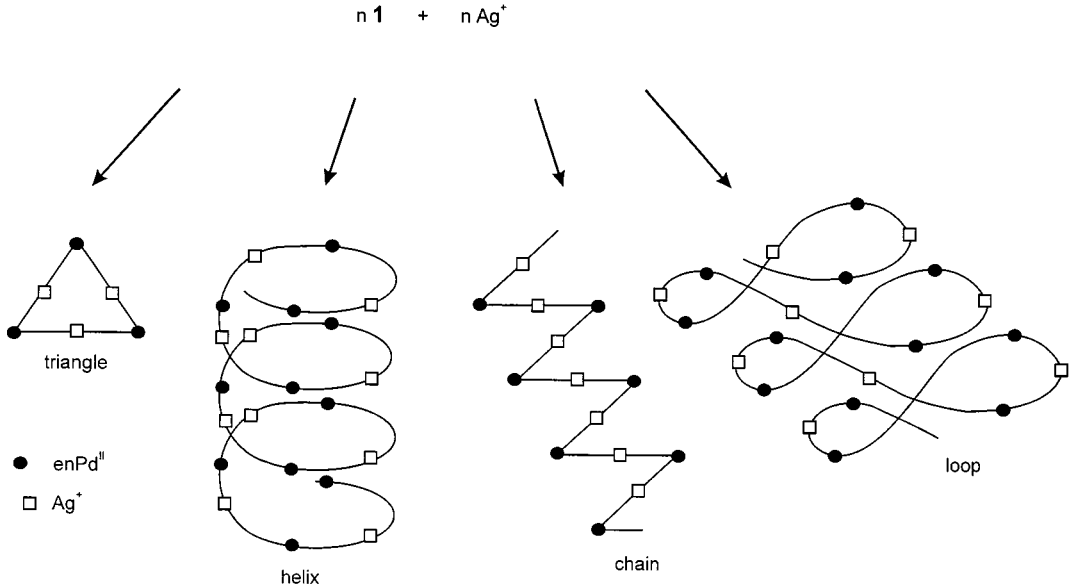

Scheme 3

N,*N*′-bis(3-pyridylmethyl)-1,4-diaminopentane], yet find formation of a 1D helix when enPt^{II} is replaced by Ag^+.[10]

Utility of *cis*-[$(H_2O)_2$M(2,2′-bpz-N^1,$N^{1'}$)]$^{2+}$ as Building Block

Our previous efforts to use 2,2′-bpz compounds had focused on coordinatively saturated enM^{II} (M = Pd or Pt) complexes with this ligand. In order to generate a molecular architecture with **1** (triangle,[6a] loop, vase[7]) bridging metal ions had to be applied. Their function was to cross-link N(4) positions. By replacing the en ligand by two Cl^- ligands, building blocks which have the potential of additional substitution of the Cl^- ligands are feasible, and hence permit an extension in two directions: Metal cross-linking through the available N(4) sites as in the case of **1** (above) and/or coordination of bridging ligands by substitution of the chloro ligands. In order to further pursue this option, we have prepared [Cl_2Pd(2,2′-bpz-N^1,$N^{1'}$)] (**4**) by reaction of K_2PdCl_4 with 2,2′-bpz and subsequently abstracted the Cl^- ligands by $AgNO_3$ to produce [$(H_2O)_2$Pd(2,2′-bpz-N^1,$N^{1'}$)]$(NO_3)_2$ (**4a**) (Scheme 4). pD-dependent ^{1}H-NMR spectra of **4a** (Figure 3) reveal formation of at least one kinetically inert (NMR time scale!) intermediate between [$(H_2O)_2$Pd(2,2′-bpz)]$^{2+}$ at low pH and the high-pH species [$(OH)_2$Pd(2,2′-bpz)]. Isolation on a preparative scale proved that this species is the dinuclear, μ-OH bridged complex [(2,2′-bpz)Pd$(OH)_2$Pd(2,2′-bpz)]$(NO_3)_2$ (**4b**). Spectra in the pD = 6−7 range indicate the presence of yet another, unidentified species. In analogy to the behavior of *cis*-[$(NH_3)_2$Pt$(H_2O)_2$]$^{2+}$,[11] [enPt$(H_2O)_2$]$^{2+}$,[12] and [enPd$(H_2O)_2$]$^{2+}$,[13] which form both μ-OH dimers, μ-OH trimers and even μ-OH tetramers,[12a] these resonances might be due to one of these higher oligomers. There is no indication of any (measurable) oligomerization of **4a** via the available N(4) sites of the 2,2′-bpz ligand.

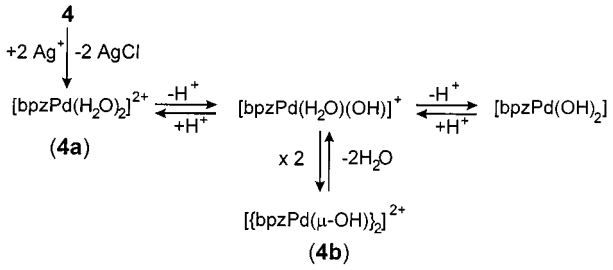

Scheme 4

The cation of [(2,2′-bpz-N^1,$N^{1'}$)Pd$(OH)_2$Pd(2,2′-bpz-N^1,$N^{1'}$)]$(NO_3)_2$·4 H_2O (**4b**) is depicted in Figure 4. Selected interatomic distances and angles are given in Table 3.

The geometry of the central PdO_2Pd core compares very well with that of the μ-OH Pt^{II} dimer mentioned above,[11a] except that the Pd···Pd separation is somewhat shorter than that of Pt···Pt. Features of the (bpz-N^1,$N^{1'}$)Pd^{II} entity are similar to those observed in related complexes.[6,7] Dinuclear cations of **4b** are arranged like the tiles of a roof in stacks with parallel 2,2′-bpz ligands approximately 3.1 Å apart. NO_3^- anions and water molecules run in channels between individual stacks and interconnect these by hydrogen-bond formation and weak axial Pd···ONO_2 contacts. For example, NO_3^- is hydrogen-bonded to a μ-OH group [2.805(4) Å], has a contact with Pd [3.370(4) Å], and forms another hydrogen bond with a water molecule [2.807(5) Å] which in turn shows a weak contact [3.38(4) Å] with C(5)H of 2,2′-bpz in a neighboring stack.

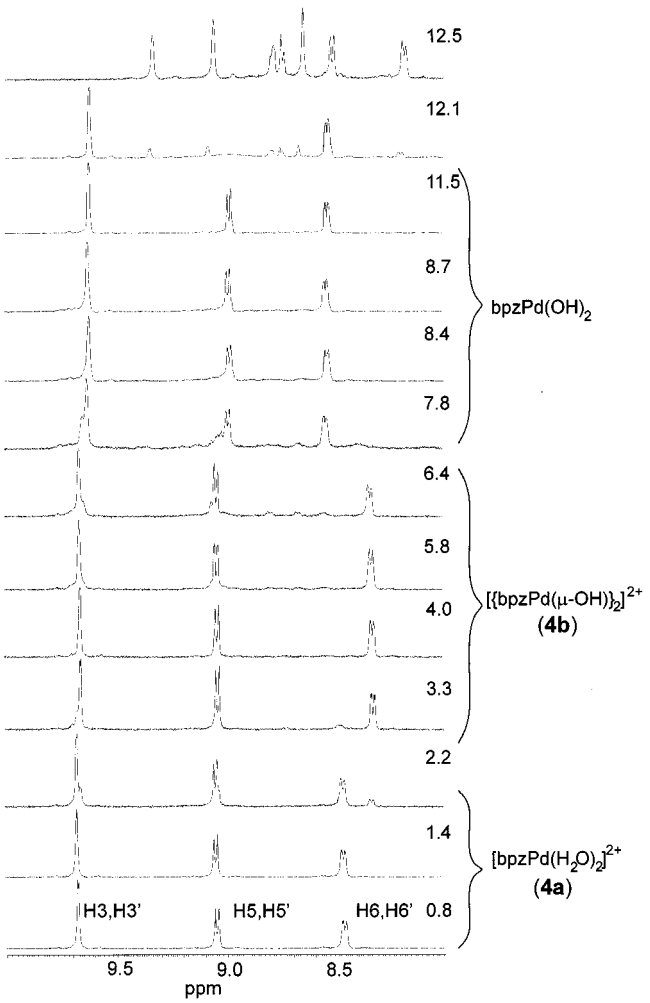

Figure 3. pD-dependent ^{1}H-NMR spectra of [(2,2′-bpz)Pd$(H_2O)_2$]$^{2+}$ in D_2O; above pD = 12 complex decomposition or rearrangement reactions take place

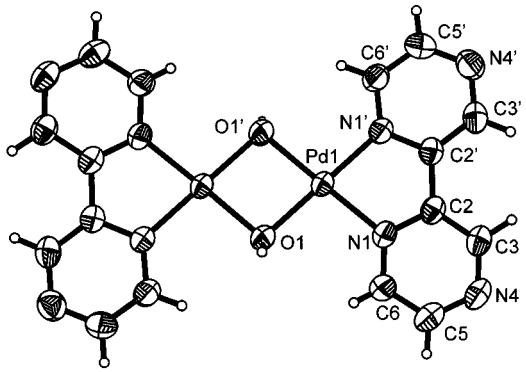

Figure 4. Molecular cation of [(2,2′-bpz-N^1,$N^{1'}$)Pd$(OH)_2$Pd(2,2′-bpz-N^1,$N^{1'}$)] $(NO_3)_2$·4 H_2O (**4b**) with atom numbering scheme; the Pt analogue **5b** is isostructural and not shown

Table 3. Selected bond lengths [Å] and angles [°] of **4b**

Pd(1)−N(1′)	1.981(3)	N(1′)−Pd(1)−N(1)	81.5(1)
Pd(1)−N(1)	1.994(2)	N(1′)−Pd(1)−O(1)[a]	178.5(1)
Pd(1)−O(1)[a]	2.005(2)	N(1)−Pd(1)−O(1)[a]	98.8(1)
Pd(1)−O(1)	2.005(2)	N(1′)−Pd(1)−O(1)	97.4(1)
Pd(1)−Pd(1)[a]	3.0185(6)	N(1)−Pd(1)−O(1)	178.6(1)
		O(1)[a]−Pd(1)−O(1)	82.3(1)
		Pd(1)[a]−O(1)−Pd(1)	97.7(1)

[a] Symmetry operation: $-x, -y, -z + 1$.

Table 4. Selected bond lengths [Å] and angles [°] of the Pt analogue of **4b**, compound **5b**

Pt(1)−N(1′)	1.960(8)	N(1′)−Pt(1)−N(1)	81.6(3)
Pt(1)−N(1)	1.975(7)	N(1′)−Pt(1)−O(1)	178.7(3)
Pt(1)−O(1)	2.009(7)	N(1)−Pt(1)−O(1)	99.6(3)
Pt(1)−O(1)[a]	2.036(7)	N(1′)−Pt(1)−O(1)[a]	98.7(3)
Pt(1)−Pt(1)[a]	3.0972(8)	N(1)−Pt(1)−O(1)[a]	179.5(3)
		O(1)−Pt(1)−O(1)[a]	80.0(3)
		Pt(1)−O(1)−Pt(1)[a]	100.0(3)

[a] Symmetry operation: $-x, -y + 2, -z + 1$.

Similarly to **4**, the corresponding Pt complex **5** was prepared, although it was not isolated in analytically pure form. Treatment of **5** with $AgNO_3$ and crystallization at pH ≈ 3 gave the isostructural Pt analogue of **4b** [(2,2′-bpz-N^1,$N^{1'}$)Pt(OH)$_2$Pt(2,2′-bpz-N^1,$N^{1'}$)](NO$_3$)$_2$·4 H$_2$O (**5b**) in crystalline form, yet low yield. The compound is not shown, but selected structural details are listed in Table 4. The purity of **5b** was also established by ^{195}Pt- as well as ^{1}H-NMR spectroscopy in D$_2$O [δ = 9.64 (s, H3, H3′), 9.02 (d, J = 4 Hz, H5, H5′), 8.88 (d, H6, H6′)]. The position of the ^{195}Pt-NMR singlet at δ = −1442 agrees well with that of the μ-OH dimer derived from (*trans*-1,2-diaminocyclohexane)Pt^{II},[14] but differs from that of *cis*-[(NH$_3$)$_2$Pt(OH)$_2$Pt(NH$_3$)$_2$]$^{2+}$ (δ = −1156).[15] Addition of DNO$_3$ (pD = 1) converts **5b** into monomeric [(D$_2$O)$_2$Pt(2,2′-bpz)]$^{2+}$ (^{1}H-NMR resonances at δ = 9.69, 9.04, 8.84), while addition of NaOD (pD = 7) in a slow reaction gives [(OH)$_2$Pt(2,2′-bpz)] (^{1}H-NMR resonances at δ = 9.49, 9.04, 8.88).

Open Molecular Box ("Square")

Conversion of **4b** to [(H$_2$O)$_2$Pd(2,2′-bpz-N^1,$N^{1'}$)]$^{2+}$ (**4a**) and subsequent reaction with 4,4′-bipyridine (4,4′-bpy) yielded the cyclic compound [{(bpz-N^1,$N^{1'}$)Pd(4,4′-bpy)}$_4$](NO$_3$)$_8$·14.4 H$_2$O (**6**) in high yield. Figure 5 gives a view of the tetranuclear cation.

Table 5. Selected bond lengths [Å] and angles [°] of **6**

Pd(1)−N(11a)	2.010(8)	N(11a)−Pd(1)−N(11b)	80.6(3)
Pd(1)−N(11b)	2.008(8)	N(11a)−Pd(1)−N(11c)	173.5(3)
Pd(1)−N(11c)	2.001(8)	N(11a)−Pd(1)−N(21d)	95.9(3)
Pd(1)−N(21d)	2.009(8)	N(11b)−Pd(1)−N(11c)	94.7(3)
		N(11b)−Pd(1)−N(21d)	175.9(4)
		N(11c)−Pd(1)−N(21d)	88.9(3)
Pd(2)−N(21a)	2.035(8)	N(21a)−Pd(2)−N(21b)	80.3(3)
Pd(2)−N(21b)	2.009(8)	N(21a)−Pd(2)−N(21c)	175.0(3)
Pd(2)−N(21c)	2.003(8)	N(21a)−Pd(2)−N(11d)[a]	96.1(3)
Pd(2)−N(11d)[a]	2.034(8)	N(21b)−Pd(2)−N(21c)	95.4(3)
		N(21b)−Pd(2)−N(11d)[a]	174.6(3)
		N(21c)−Pd(2)−N(11d)[a]	88.4(3)

[a] Symmetry operation: $-x + 1, -y, -z + 2$.

Salient structural features are listed in Table 5. The cation bears a close resemblance to related molecular squares[16] built of 4,4′-bpy sides and segments of two-dimensional networks containing the 4,4′-bpy square motif, respect-

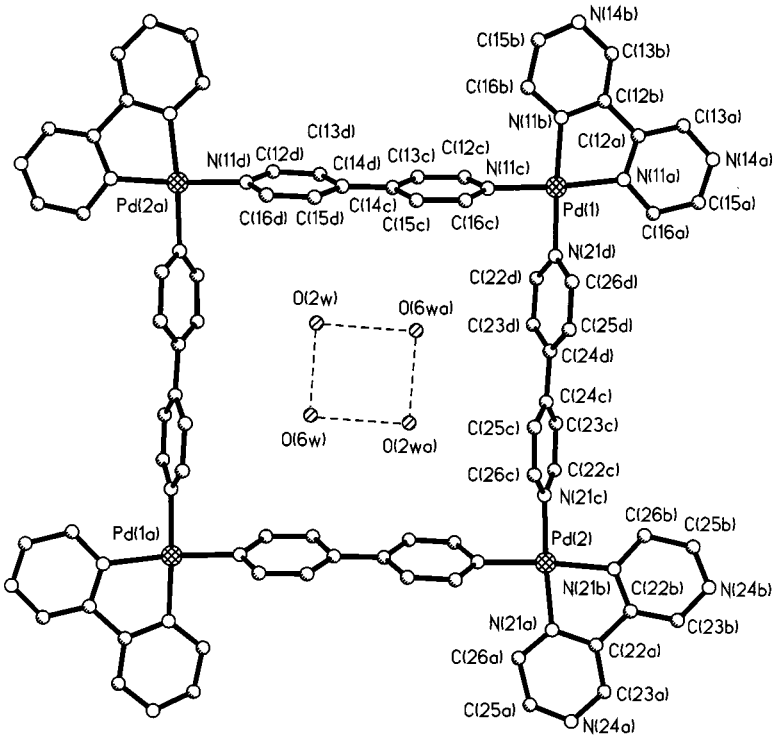

Figure 5. View of tetranuclear cation of **6** with four water molecules inserted

ively.[17] The four heavy-metal ions are exactly coplanar (as opposed to a strongly puckered, hence nonplanar arrangement as seen with bulky phosphane groups at the metal entities[16]), forming a square with edge-to-edge distances of ca. 11.057(3) Å and diagonal Pd···Pd distances of 15.703(4) Å [Pd(1)···Pd(1)] and 15.603(4) Å [Pd(2)···Pd(2)]. Of the 4,4′-bpy units in **6**, two are markedly twisted [41.6(3)°] about the central C−C bond, while the two others are hardly twisted [1.5(7)°]. Nevertheless, the four 4,4′-bpy ligands are approximately perpendicular to the Pd_4 square, thus making **6** in essence an "open box".[18] The coordination geometries of the Pd corner units deviate markedly from the ideal square-plane as far as angles are concerned. Four water molecules, interacting through H bonds [O(2w)···O(6w), 2.97(2) Å] and almost coplanar with the Pd_4 plane [deviations 0.26(2) Å for O(2w); 0.25(2) Å for O(6w)], reside in the center of the square. Tetranuclear cations of **6** stack, at a distance of 6.302(1) Å between Pd centers, in such a way as to produce long channels (Figure 6), which run along the *y* axis. Individual segments of the channel (Pd_4 squares) are interrupted by four NO_3^- anions, which are oriented parallel to the Pd_4 plane and sandwiched between individual squares. Pd···O distances are 3.02(1) Å [Pd(1)···O(22)] and 3.09(1) Å [Pd(2)···O(12)]. The remaining anions are distributed as follows: Pairs of NO_3^- anions (50% occupancy) are oriented perpendicular to the Pd_4 planes in the space between layers of Pd_4 squares. They show multiple hydrogen bonding interactions with additional water molecules. The remaining NO_3^- anions (three per tetranuclear cation) reside at the outside of the square, hence between individual channels.

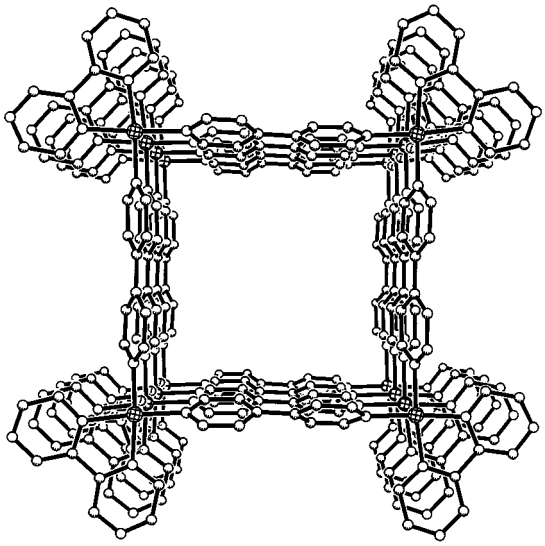

Figure 6. Packing diagram with channel formed by cations of **6**; the view is along the *y* axis; nearest intercationic Pd···Pd distances are 6.302(1) Å; water molecules and NO_3^- anions are omitted

Formation of similar channels has been reported before,[16,17,19] occasionally with inclusion of strongly hydrophobic guests such as *o*-halobenzene[17] or naphthalene.[19]

In aqueous solution (pD = 2) **6** coexists with a second species. In addition to the five ^{1}H-NMR resonances due to the 2,2′-bpz ligands (H3, H3′; H5, H5′; H6, H6′) and the two protons H_α and H_β of 4,4′-bpy, a second set of resonances (ca. 30−35% of the former at a concentration of 0.016 M of dissolved tetramer **6**) is observed. The assignment of the individual resonances is straightforward on the basis of differences in H,H coupling constants and 2D-NMR experiments, respectively. The simplicity of the signal patterns of 2,2′-bpz and 4,4′-bpy resonances of both species present in solution are neither consistent with dissociation of tetranuclear **6** into monomeric $[(2,2'\text{-bpz})Pd(4,4'\text{-bpy-}N^1)(D_2O)]^{2+}$ (expected doubling of bpz and bpy resonances due to nonequivalence of two halves of these molecules) nor dissociation into $[(2,2'\text{-bpz})Pd(4,4'\text{-bpy-}N^1)_2]^{2+}$ and free $[(2,2'\text{-bpz})Pd(D_2O)_2]^{2+}$ (expected doubling of bpy resonances; two sets of bpz resonances). We tentatively favor a proposal made by Fujita et al.,[19] according to which the molecular square assembled from $(2,2'\text{-bpy})Pd^{II}$ (2,2′-bpy = 2,2′-bipyridine) and 4,4′-bpy equilibrates in solution with a cyclic trinuclear species[19] (Scheme 5). An interesting detail of the ^{1}H-NMR spectrum of dissolved **6** (c.f. Experimental Section) supporting this view refers to the chemical shift of the protons H6, H6′ of the 2,2′-bpz ligands in the two species: In the major species, which is assigned to the square, this resonance (d, $^3J_{5,6}$ = 3 Hz) occurs at δ = 7.98 while in the minor one, tentatively assigned to the cyclic trimer, this doublet is found at δ = 8.38. From model building it becomes clear that H6, H6′ of 2,2′-bpz is experiencing the ring current of the pyridine ring of the 4,4′-bpy ligands to a larger extent than is to be anticipated for a triangular structure. Therefore it is to be expected that H6, H6′ of 2,2′-bpz resonates upfield from that of the molecular triangle in the case of a molecular square.

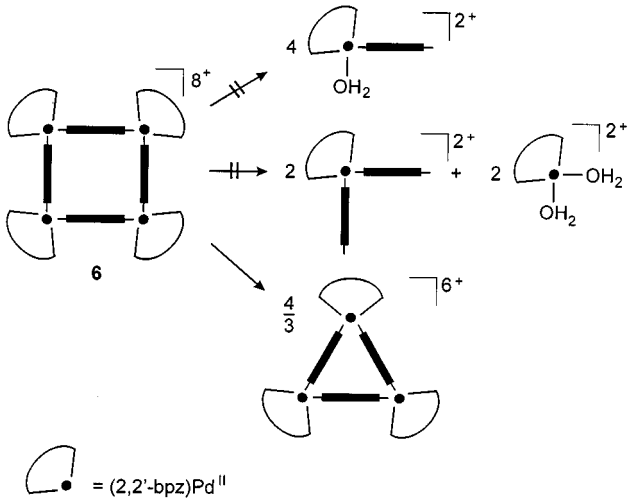

Scheme 5

Conclusions

As outlined in Scheme 6, $[L_2Pd(2,2'\text{-bpz-}N^1,N^{1'})]^{2+}$ cations [L_2 = en (**1**), L = H_2O (**4a**)] represent useful angular units for the generation of larger cationic aggregates. There are two principal ways by which this can be achieved. (i) When additional metal ions M′ bind to the available N(4) positions of the chelating 2,2′-bpz ligand in **1** and cross-

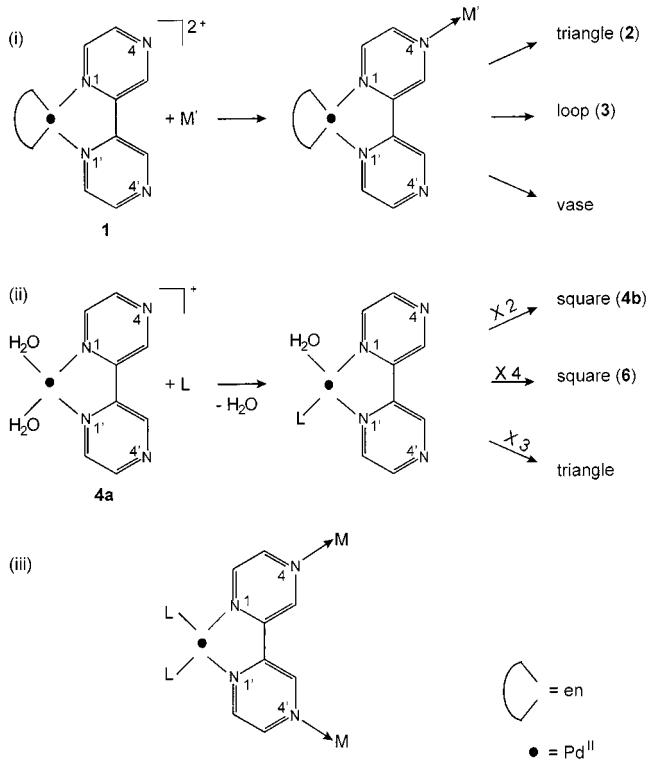

Scheme 6

link to other cations **1**, depending on the geometry of M′, flat triangles [M′ = *trans*-$(NH_3)_2Pt^{II}$ **2**[6c]], loop structures ($M' = Ag^+$ in **3**) or hexanuclear vases (M′ = $enPd^{II}$ [7]) can form. (ii) Compound **4a** can likewise act as an angular unit upon substitution of the aqua ligands by other bridging ligands L. These may be small (OH^- in **4b**) or large (4,4′-bpy in **6**) and may themselves be angular (OH^-) or linear units (4,4′-bpy). Of course, variations of these motifs are possible, e.g. upon use of M′−L−M′ fragments in (i) or L−M′−L linear units in (ii). Finally there is, in principle, also the possibility of combining (i) and (ii) in such a way as to use **4a** as a cross element in molecular architecture [option (iii) in Scheme 6].

Experimental Section

2,2′-Bpz[20] and [enPd(2,2′-bpz-$N^1,N^{1'}$)]$(ClO_4)_2$ (**1**)[6a] were prepared as reported. 4,4′-Bipyridine was obtained commercially.

[enPd(2,2′-bpz-$N^1,N^{1'}$)Ag]$_n(ClO_4)_{3n}$ (3): [enPd(2,2′-bpz-$N^1,N^{1'}$)]$(ClO_4)_2$ (**1**) (100.00 mg, 0.191 mmol) was dissolved in water (10 mL) and stirred with $AgClO_4$ (43.00 mg, 0.191 mmol) for 1 d at room temperature. The yellow solution was then filtered, concentrated to 3 mL by rotary evaporation, and then kept at 4 °C. Yellow **3** was obtained in 79% yield (110.28 mg) within 4 d. $C_{10}H_{14}AgCl_3N_6O_{12}Pd$ (730.89): calcd. C 16.4, H 1.9, N 11.4; found C 16.2, H 1.9, N 11.3. ***Caution!*** Perchlorate salts are potentially explosive and should be used in small quantities only.

[Cl_2Pd(2,2′-bpz-$N^1,N^{1'}$)] (4): 2,2′-bpz (100.00 mg, 0.63 mmol) and K_2PdCl_4 (206.00 mg, 0.63 mmol) were suspended in water (20 mL) and stirred for 1 d at room temperature. The yellow solid was then filtered off and washed with $CHCl_3$ (10 mL) (95% yield, 200.78 mg). $C_8H_6Cl_2N_4Pd$ (335.48): calcd. C 28.6, H 1.8, N 16.7; found C 28.3, H 1.9, N 16.5.

[$(H_2O)_2$Pd(2,2′-bpz-$N^1,N^{1'}$)]$(NO_3)_2$ (4a): The complex was prepared in situ by treating **4** with 2 equiv. of $AgNO_3$ in H_2O or alternatively by acidification (HNO_3, pH < 3) of an aqueous solution of **4b**. − ^{1}H NMR (200 MHz, D_2O, TSP, pD < 3): δ = 8.47 (dd, $^3J_{5,6}$ = 3 Hz, 2 H, arom., $^5J_{3,6}$ = 1.1 Hz, 2 H, arom.), 9.05 (d, $^3J_{5,6}$ = 3 Hz, 2 H, arom.), 9.68 (d, $^5J_{3,6}$ = 1 Hz, 2 H, arom.).

[(2,2′-bpz-$N^1,N^{1'}$)Pd$(OH)_2$Pd(2,2′-bpz-$N^1,N^{1'}$)]$(NO_3)_2$·4 H_2O (4b): **4** (300.00 mg, 0.994 mmol) was suspended in water (15 mL) and stirred for 24 h at room temperature with $AgNO_3$ (338.00 mg, 1.988 mmol). After removal of AgCl by filtration, the pH value was adjusted to 3, then the reaction mixture was heated to 60 °C and filtered again. Yellow-orange crystals of **4b** were isolated in 62% yield (222.85 mg) within 1 d at 4 °C. $C_{16}H_{18}N_{10}Pd_2O_{10}$ (723.21 for dihydrate): calcd. C 26.6, H 2.5, N 19.4; found C 26.7, H 2.4, N 19.3. − ^{1}H NMR (200 MHz, D_2O, TSP, pD = 5.5): δ = 8.34 (dd, $^3J_{5,6}$ = 3 Hz, 2 H, arom., $^5J_{3,6}$ = 1.1 Hz, 2 H, arom.), 9.05 (d, $^3J_{5,6}$ = 3 Hz, 2 H, arom.), 9.66 (d, $^5J_{3,6}$ = 1 Hz, 2 H, arom.).

[Cl_2Pt(2,2′-bpz-$N^1,N^{1'}$)] (5): 2,2′-bpz (100.00 mg, 0.63 mmol) and K_2PtCl_4 (262.00 mg, 0.63 mmol) were suspended in water (15 mL) and stirred for 4 d at 80 °C. The yellow solid was then filtered off, washed with $CHCl_3$ (10 mL) and dried. **5** could not be isolated in pure form and possibly contained a compound with (2,2′-bpz-$N^4,N^{4'}$)Pt^{II} species.

[(2,2′-bpz-$N^1,N^{1'}$)Pt$(OH)_2$Pt(2,2′-bpz-$N^1,N^{1'}$)]$(NO_3)_2$·4 H_2O (5b): Crude **5** (369.00 mg, 0.87 mmol) was suspended in water (15 mL) and stirred for 24 h at 80 °C with $AgNO_3$ (338.00 mg, 1.988 mmol). After removal of AgCl by filtration, the pH value was adjusted to 3, the reaction mixture heated to 60 °C and filtered again. Yellow-orange crystals of **5b** were isolated in less than 5% yield (22.00 mg)

Table 6. X-ray data for **3**, **4b**, **5b**, and **6**

	3	**4b**	**5b**	**6**
Empirical formula	$C_{10}H_{14}AgCl_3N_6O_{12}Pd$	$C_8H_{11}N_5O_6Pd$	$C_8H_{11}N_5O_6Pt$	$C_{36}H_{42.4}N_{16}O_{19.2}Pd_2$
Molecular mass	730.89	379.62	468.31	1219.26
Space group	*Pbcn*	$P2_1/n$	$P2_1/n$	$P2_1/n$
a [Å]	17.946(4)	7.0430(10)	7.0440(10)	27.231(5)
b [Å]	17.616(4)	23.222(5)	23.100(5)	6.3020(10)
c [Å]	13.559(3)	7.893(2)	7.985(2)	27.273(5)
β [°]		106.22(3)	106.68(3)	91.02(3)
V [Å^3]	4286.5(17)	1239.5(4)	1244.6(4)	4679.6(14)
Z	8	4	4	4
T [K]	293(2)	293(2)	293(2)	293(2)
μ [mm^{-1}]	2.200	1.533	11.310	0.863
R_1 (obs. data)[a]	0.0361	0.0276	0.0374	0.0661
wR_2 (obs. data)[b]	0.0904	0.0634	0.0913	0.1416

[a] $R_1 = \Sigma \, ||F| - |F_c|| / \Sigma \, |F|$. − [b] $wR_2 = [\Sigma w(F^2 - F_c^2)^2 / \Sigma w(F^2)^2]^{1/2}$.

within 1 d at 4 °C. − ^{1}H NMR (200 MHz, D_2O, TSP, pD = 4.2): δ = 8.71 (d, $^3J_{5,6}$ = 4 Hz, 2 H, arom.), 9.02 (d, $^3J_{5,6}$ = 4 Hz, 2 H, arom.), 9.62 (s, 2 H, arom.).

[{(2,2′-bpz-N^1,$N^{1'}$)Pd(4,4′-bpy)}$_4$](NO$_3$)$_8$·14.4 H$_2$O (6): 4b (88.00 mg, 0.127 mmol) was dissolved in H_2O (15 mL) at 40 °C and the pH value of the solution was adjusted to 1.5 with 1N HNO_3. 4,4′-Bipyridine (38.00 mg, 0.243 mmol) was then added, the pH value readjusted and the mixture stirred for 12 h at 45 °C. Following cooling at 4 °C, thin yellow needles of **6** were isolated within 1 h. The needles were filtered and washed with H_2O (5 mL). After recrystallization from H_2O, the yield was 86% (132.60 mg). $C_{72}H_{84.8}N_{32}Pd_4O_{38.4}$ (2438.52): calcd. C 35.5, H 3.5, N 18.4; found C 35.9, H 3.2, N 18.8. − ^{1}H NMR (200 MHz, D_2O, TSP, pD = 2) major peaks: δ = 10.17 (s, 2 H, arom. H3-bpz), 9.60 (d, $^3J_{\alpha,\beta}$ = 6.5 Hz, 4 H, arom. Hα-bpy), 9.24 (d, $^3J_{5,6}$ = 3 Hz, 2 H, arom. H5-bpz), 8.49 (d, $^3J_{\alpha,\beta}$ = 6.5 Hz, 4 H, arom. Hβ-bpy), 7.98 (d, $^3J_{5,6}$ = 3 Hz, 2 H, arom. H6-bpz); minor peaks: δ = 9.41 (d, $^3J_{\alpha,\beta}$ = 6.5 Hz, 4 H, arom. Hα-bpy), 9.29 (d, $^3J_{5,6}$ = 3 Hz, 2 H, arom. H5-bpz), 8.38 (d, $^3J_{5,6}$ = 3 Hz, 2 H, arom. H6-bpz), 8.35 (d, $^3J_{\alpha,\beta}$ = 6.5 Hz, 4 H, arom. Hβ-bpy).

Instrumentation: ^{1}H-NMR spectra were recorded at 20 °C with a Bruker AC 200 FT NMR spectrometer in D_2O (with TSP as internal standard). pD values (for D_2O solutions) were obtained by adding 0.4 units to the pH meter reading of the electrode. − Elemental analyses were performed with a Carlo Erba Model 1106 Strumentazione Element-Analyzer.

X-ray Crystal Structure Determinations: Intensity data for **3**, **4b**, **5b**, and **6** were collected with an Enraf−Nonius Kappa CCD[21] (Mo-K_α, λ = 0.71069 Å, graphite monochromator) with sample-to-detector distances of 26.7 (**4b**, **5b**), and 30.7 mm (**3**, **6**), respectively. They covered the whole sphere of reciprocal space by measurement of 360 frames rotating about ω in steps of 1°. The exposure times were 14 (**3**), 30 (**4b**), 45 (**5b**), and 75 s (**6**) per frame. Preliminary orientation matrices and unit cell parameters were obtained from the peaks of the first ten frames, respectively, and refined using the whole data set. Frames were integrated and corrected for Lorentz and polarization effects using DENZO.[22] The scaling as well as the global refinement of crystal parameters were performed by SCALEPACK.[22] Reflections, which were partly measured on previous and following frames, are used to scale these frames with each other. Merging of redundant reflections in part eliminates absorption effects and also reveals if crystal decay occurs. The structures were solved by standard Patterson methods[23] and refined by full-matrix least squares based on F^2 using the SHELXTL-PLUS[24] and SHELXL-93 programs.[25] The scattering factors for the atoms were those given in the SHELXTL-PLUS program. Transmission factors were calculated with SHELXL-97.[26] Hydrogen atoms were included in calculated positions and refined with isotropic displacement parameters according to the riding model, except for all protons in **4b** and the hydroxy and the four water protons in **5b**, which could be localized with difference Fourier synthesis. The anions and water molecules in **3** and **6** are disordered.[27] X-ray data are provided in Table 6.

Acknowledgments

This work was supported by the Fonds der Chemischen Industrie.

[1] J.-M. Lehn, *Supramolecular Chemistry*, VCH, Weinheim, **1995**. − P. J. Stang, *Chem. Eur. J.* **1998**, *4*, 19. − M. Fujita, K. Ogura, *Coord. Chem. Rev.* **1996**, *148*, 249. − R. W. Saalfrank, I. Bernt, *Curr. Opin. Solid State Mat. Sci.* **1998**, *3*, 407. − D. L. Caulder, K. N. Raymond, *J. Chem. Soc., Dalton Trans.* **1999**, 1185.
[2] J. A. R. Navarro, B. Lippert, *Coord. Chem. Rev.* **1999**, *185−186*, 653.
[3] M. S. Lüth, E. Freisinger, F. Glahé, B. Lippert, *Inorg. Chem.* **1998**, *37*, 5044.
[4] H. Rauter, I. Mutikainen, M. Blomberg, C. J. L. Lock, P. Amo-Ochoa, E. Freisinger, L. Randaccio, E. Zangrando, E. Chiarparin, B. Lippert, *Angew. Chem. Int. Ed. Engl.* **1997**, *36*, 1296.
[5] H. Rauter, E. C. Hillgeris, B. Lippert, *J. Chem. Soc., Chem. Commun.* **1992**, 1385. − H. Rauter, E. C. Hillgeris, A. Erxleben, B. Lippert, *J. Am. Chem. Soc.* **1994**, *116*, 616. − J. A. R. Navarro, M. B. L. Janik, E. Freisinger, B. Lippert, *Inorg. Chem.* **1999**, *38*, 426.
[6] [6a]R.-D. Schnebeck, L. Randaccio, E. Zangrando, B. Lippert, *Angew. Chem. Int. Ed.* **1998**, *37*, 119. − [6b]R.-D. Schnebeck, E. Freisinger, B. Lippert, *Angew. Chem. Int. Ed.* **1999**, *38*, 168. − [6c]R.-D. Schnebeck, E. Freisinger, B. Lippert, *J. Chem. Soc., Chem. Commun.* **1999**, 675.
[7] R.-D. Schnebeck, E. Freisinger, F. Glahé, B. Lippert, *J. Am. Chem. Soc.* **2000**. *122*, 1381.
[8] T. Suzuki, H. Kotsuki, K. Isobe, N. Moriya, Y. Nakagawa, M. Ochi, *Inorg. Chem.* **1995**, *34*, 530. − L. Carlucci, G. Ciani, D. M. Proserpio, A. Sironi, *Inorg. Chem.* **1998**, *37*, 5941. − N. Masciocchi, G. A. Ardizzoia, G. LaMonica, A. Maspero, A. Sironi, *Angew. Chem. Int. Ed.* **1998**, *37*, 3366.
[9] D. Whang, K.-M. Park, J. Heo, P. Ashton, K. Kim, *J. Am. Chem. Soc.* **1998**, *120*, 4899.
[10] D. Whang, J. Heo, C.-A. Kim, K. Kim, *Chem. Commun.* **1997**, 2361.
[11] [11a] R. Faggiani, B. Lippert, C. J. L. Lock, B. Rosenberg, *J. Am. Chem. Soc.* **1977**, *99*, 777. − [11b] R. Faggiani, B. Lippert, C. J. L. Lock, B. Rosenberg, *Inorg. Chem.* **1977**, *16*, 1192. − [11c] R. Faggiani, B. Lippert, C. J. L. Lock, B. Rosenberg, *Inorg. Chem.* **1978**, *17*, 1941. − [11d] B. Lippert, C. J. L. Lock, B. Rosenberg, M. Zvagulis, *Inorg. Chem.* **1978**, *17*, 2971.
[12] [12a] F. D. Rochon, A. Morneau, R. Melanson, *Inorg. Chem.* **1988**, *27*, 10. − [12b] F. D. Rochon, R. Melanson, *Acta Crystallogr.* **1988**, *C44*, 474.
[13] R. B. Martin *in Cisplatin: Chemistry and Biochemistry of a Leading Anticancer Drug* (Ed.: B. Lippert), VHCA and Wiley-VCH, Weinheim, **1999**, p. 183−205.
[14] D. S. Gill, B. Rosenberg, *J. Am. Chem. Soc.* **1982**, *104*, 4598.
[15] B. Rosenberg, *Biochimie* **1978**, *60*, 859. − S. J. Lippard, *Science* **1982**, *218*, 1075.
[16] P. J. Stang, D. H. Cao, S. Saito, A. M. Arif, *J. Am. Chem. Soc.* **1995**, *117*, 6273.
[17] M. Fujita, Y. J. Kwon, S. Washizu, K. Ogura, *J. Am. Chem. Soc.* **1994**, *116*, 1151.
[18] We use the term "square" in this context, because it had been introduced by Fujita and Ogura[17] as well as Stang et al.[16] For "squares" with flat organic corner stones see, e.g., ref.[3]
[19] M. Fujita, O. Sasaki, T. Mitsuhashi, T. Fujita, J. Yazaki, K. Yamaguchi, K. Ogura, *Chem. Commun.* **1996**, 1535.
[20] R. J. Crutchley, A. B. P. Lever, *Inorg. Chem.* **1982**, *21*, 2276.
[21] NONIUS BV, KappaCCD package, Röntgenweg 1, P. O. Box 811, 2600 AV Delft, Netherlands.
[22] Z. Otwinowsky and W. Minor, *Methods Enzymol.*, **1996**, *276*, 307.
[23] G. M. Sheldrick, *Acta Crystallogr.* **1990**, *A46*, 467.
[24] G. M. Sheldrick, *SHELXTL-PLUS (VMS)*, Siemens Analytical X-ray Instruments, Inc.: Madison, WI, **1990**.
[25] G. M. Sheldrick, *SHELXL-93, Program for crystal structure refinement*, University of Göttingen, Germany, **1993**.
[26] G. M. Sheldrick, *SHELXL-97, Program for the refinement of crystal structures*, University of Göttingen, Germany, **1997**.
[27] Crystallographic data (excluding structure factors) for the structure reported in this paper have been deposited with the Cambridge Crystallographic Data Centre as supplementary publication no. CCDC-137745 to CCDC-137748. Copies of the data can be obtained free of charge on application to CCDC, 12 Union Road, Cambridge CB2 1EZ, UK [Fax: (internat.) + 44-1223/336-033; E-mail: deposit@ccdc.cam.ac.uk].

Received December 15, 1999
[I99461]